ENVIRONMENTAL STUDIES

Offshore wind: An opportunity for cost-competitive decarbonization of China's energy economy

Peter Sherman[1], Xinyu Chen[2,3]*, Michael McElroy[1,3]*

China has reduced growth in its emissions of greenhouse gases, partly attributable to major investments in on-shore wind. By comparison, investments in offshore wind have been minor, limited until recently largely by perceptions of cost. Assimilated meteorological data are used here to assess future offshore wind potential for China. Analysis on a provincial basis indicates that the aggregate potential wind resource is 5.4 times larger than the current coastal demand for power. Recent experiences with markets in both Europe and the United States suggest that potential offshore resources in China could be exploited to cost-competitively provide 1148.3 TWh of energy in a high-cost scenario, 6383.4 TWh in a low-cost option, equivalent to between 36 and 200% of the total coastal energy demand after 2020. The analysis underscores notable benefits for offshore wind for China, with prospects for major reductions in greenhouse emissions with ancillary benefits for air quality.

INTRODUCTION

Under the Paris Agreement, the Chinese government pledged to supply 20% of its primary energy consumption with renewables by 2030. Renewable resources are expected to provide approximately 40% of its electricity generation by that time (*1*). China's installed capacity for onshore wind has expanded substantially since the start of the 21st century, growing from 0.3 GW of cumulative wind power capacity in 2000 to roughly 162 GW in 2017 (*2*). The pace of this growth is unprecedented and has established China as the world leader in onshore wind investment. While renewable energy represents a small fraction of China's current overall energy consumption [11% in 2016 (*3*)], the trajectory of onshore wind has helped pave an important path to a potential future decarbonized—or decarbonizing—China.

Despite hopeful prospects for China's onshore wind, expectations have been somewhat tempered over the past few years. There are a number of issues associated with onshore wind in China that limit its utility. Curtailment of wind-generated electricity poses a major limitation for China's onshore power production (*4*). The Brookings-Tsinghua Center for Public Policy estimates that 16% of total potential wind generation was curtailed at a cost of more than $1.2 billion between 2010 and 2016 (*3*). In addition, China's onshore wind market faces a further challenge of geographic imbalance; the greatest wind resource is located far from the high-demand, population-dense regions of the country. Provinces in the coastal zone consume approximately 80% of total national electricity, which is problematic given that the vast majority of the installed capacity for onshore wind is separated by a distance of more than 1000 miles. Another area of potential concern relates to the declining temporal trend in land wind speeds over high-resource regions such as Inner Mongolia. This secular decrease has been identified in reanalysis data (*5*), in climate models (*6–9*), and in observations (*10, 11*). It is suggested that some of the decline may be attributed to a weakening of the land-sea temperature gradient associated with global climate change (*12*). If the declining

trend were to continue—as has been indicated in Coupled Model Intercomparison Project Phase 5 (CMIP5) projections under both medium- and high-emissions scenarios—then climate change might be expected to reduce the financial return on both current and future investments in China's onshore wind (*13*). Offshore wind offers an alternative that might mitigate many of these issues and is already an important component in energy plans for a number of countries, notably in Europe but with strong potential for the United States as well.

Currently, Europe is the largest investor in offshore wind, with the United Kingdom, Germany, Denmark, Netherlands, and Belgium ranking as five of the top six countries in terms of installed capacity (*14, 15*). Close to 90% of the presently installed global capacity for offshore wind is located in the North Sea and in neighboring regions of the Atlantic Ocean (*15*). There is important room though for growth; cumulative installed capacity for offshore wind accounted for just 3.7% of global investments in wind capacity in 2017 (*15*). These numbers are likely to change, however, in the not-too-distant future. Technological improvements have raised capacity factors (CFs) for offshore wind systems with decreases in both fixed and variable costs combined with installation of larger turbines that increase energy output (*14*). Costs have plummeted, highlighted by a decline of approximately 30% in mean installed costs between 2013 and 2018 (*15*). The recent 800-MW offshore wind farm approved for Massachusetts indicates that the trend exhibited in Europe is poised to extend to the United States. That facility is projected to deliver power at a cost of $0.074 kWh^{-1} in its initial phase, decreasing later to $0.065 kWh^{-1}, such that the investment is immediately competitive with current sources fueled primarily by coal and natural gas (*16*).

Given the technological improvements and the expansion of the market beyond Europe, there is reason to believe that offshore wind power may be economically viable also for China. China's current offshore installed capacity is low, representing only 1.6% of the country's total commitment to wind power. The primary reason for China's small offshore wind investment is the perception of cost, i.e., that other renewables are cheaper. However, recent expansion of offshore wind in Europe and the United States (discussed above) indicates that the economics of offshore wind has changed markedly recently and could be cost-competitive now with present technologies. In addition, barriers that have historically inhibited construction of offshore wind in the United States may not pose comparable problems for China. For

[1]Department of Earth and Planetary Sciences, Harvard University, Cambridge, MA 02138, USA. [2]State Key Laboratory of Advanced Electromagnetic Engineering and Technology, School of Electrical and Electronic Engineering, Huazhong University of Science and Technology, Wuhan 430074, China. [3]John A. Paulson School of Engineering and Applied Sciences, Harvard University, Cambridge, MA 02138, USA.
*Corresponding author. Email: mbm@seas.harvard.edu (M.M.); xchen2019@hust.edu.cn (X.C.)

example, the Cape Wind Project in Massachusetts was subjected to objections and delays due in part to concerns that offshore turbines would obstruct scenic views of Nantucket Sound and introduce obstacles that ferries would need to avoid. A major difference between China and the United States is that China's coastline is largely government property, implying that many of the objections to offshore wind in the United States would not be applicable in China. In addition, shallow waters surrounding China's coast extend much further offshore relative to the situation in the United States, allowing for a larger area suitable for offshore turbines. In any event, we believe that the issues that have delayed offshore wind development in the United States are unlikely to be consequential in China. While extensive discussions for China have focused on resource availability, economics, and the utilization of onshore wind power (1–5, 17), little attention has been devoted to the possibility of using offshore wind resources to decarbonize coastal energy systems. Lu et al. (18) assessed the energy density for offshore wind power, but the economics of offshore wind power were not addressed. Hong and Möller (19) offered important assessments of economic feasibility considering practical geographic constraints but did not account for the exclusion of environmental protection zones, nor did it allow for water-depth restrictions. In addition, consideration of economics and the practicalities of grid integration on a provincial level were not included. The aforementioned studies were based on the technical and economic status of offshore wind turbine before 2013, when the typical CF was 37%, levelized cost was above $0.20 kWh^{-1}, and turbines could only be installed in shallow waters near shore.

The objective of this paper is to explore the potential for offshore wind power for coastal provinces in China taking advantage of insights based on the most recent technological and economic data. The offshore wind potential is assessed at a spatial resolution of 0.03° by 0.03° on the basis of assimilated wind speeds derived from NASA's MERRA-2 (Modern-Era Retrospective analysis for Research and Applications, version 2) rescaled to a high-resolution bathymetry dataset (see Materials and Methods for details). Data are filtered according to

water depth, ocean territories, environmental protection zones, and competing demands for the use of shipping lanes. Economic feasibility is evaluated on the basis of current and projected costs, accounting for water depth, distance to shore, and wind quality. The hourly, seasonal, and interannual variability of offshore wind power is investigated using a 39-year record of assimilated hourly wind speeds. Implications for integrating offshore wind power into different provincial power systems are analyzed and discussed. The calculations provide a guide for investments in offshore wind that could be economically justified for individual provinces. The analysis indicates that a large portion of the region's current and future power demand could be provided cost-effectively through investments in offshore wind.

RESULTS
China has abundant offshore wind resources
CFs are calculated on the basis of MERRA-2 wind speeds over the full 39-year period using an adapted method for on- and offshore wind power. Geographical regions were filtered according to water depths of less than 60 m with exclusion of environmentally protected areas and shipping lanes (discussed in Materials and Methods). Data were restricted to regions within China's Exclusive Economic Zone (EEZ) boundary (the environment under which a coastal state assumes jurisdiction over its neighboring marine resources; see Materials and Methods). Hourly mean values of CF and levelized cost of electricity (LCOE) over feasible locations for China's offshore wind are displayed in Fig. 1 (the SD distribution is shown in fig. S1).

Notably, areas with the largest CFs do not overlap those with low LCOE, implying that distance to shore and depth are important considerations for siting offshore locations. The economics of offshore wind will be discussed further in the next subsection. Provincial jurisdictions of ocean regions are delineated by the dashed blue boundaries. The greatest offshore wind resource is seen off the coast of Fujian, followed by opportunities identified with Zhejiang, Guangdong, Shanghai, and Hainan. The energy generation potential for some of these large
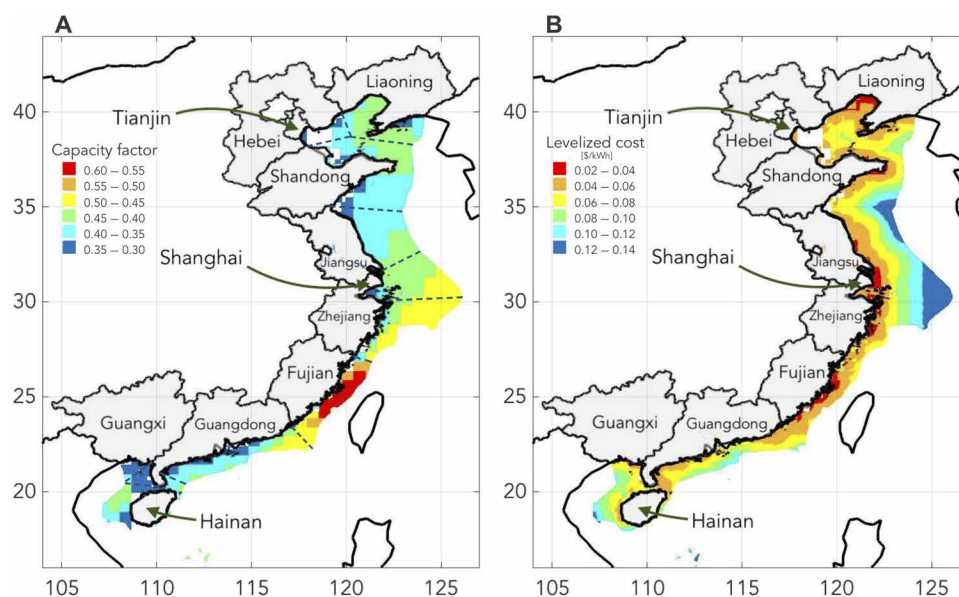

Fig. 1. CFs and levelized costs of electricity. Spatial distributions of the mean (**A**) CF and (**B**) LCOE ($ kWh^{-1}) over 1980–2018 for the filtered region. Coastal provinces are colored gray. The dashed blue lines denote offshore wind areas that are in closest proximity to particular provinces. Note the different color bar limits in (A) and (B).

resource regions is constrained primarily by EEZ boundaries. Fujian has one of the lowest potential offshore capacities among all of the coastal provinces considered here (see Table 1) despite its extensive coastal boundary; its waters are shared with Taiwan. Liaoning, by comparison, competes for wind resources with three other provinces and with North Korea despite the fact that it has similar offshore capacity (Table 1). Notably, the mean wind resource over most of the coastal region is much greater than China's onshore average [i.e., comparison of Fig. 1A with fig. 1a from (5)]. Given that the environments with optimal offshore wind resources are much closer to population-dense regions as compared with the most favorable locations for onshore facilities, this provides a compelling argument for the viability of China's offshore wind resources.

Offshore wind will be cost-competitive by 2030, and may already be

From the above analysis, it is clear that China has a large physical potential for offshore wind. The next step in our analysis is to assess the economic costs associated with the development of offshore wind and to compare related levelized costs with competing costs for current sources of power from coal and nuclear. Results of the cost analysis are summarized in Fig. 2.

We considered two cost scenarios for 2020: high ($3500 kW^{-1}) and low ($2000 kW^{-1}), based on the range of results for offshore wind farms deployed in 2018 as indicated in the report published by the International Renewable Energy Agency (IRENA) (2). These costs were adjusted according to water depth and distance from shore (see the Materials and Methods for further details). We projected costs to 2030 as well, using the 30% LCOE decline predicted by Wiser et al. (20). From the provincial breakdown, it is clear that the cost-efficient capacity in the high-cost scenario is regionally variable. For example, 388.9 TWh could be supplied economically in Jiangsu, while opportunities in Guangdong would be minimal (Table 2), despite the fact that the two provinces have comparable physical potentials (Table 1). The variability is less of an issue in the low-cost scenario, where the capacity of cost-competitive electricity exceeds demand in all nine of the coastal provinces included in Table 2. The cost-competitive capacity that could be realized in this scenario is 200% larger than current overall peak demands for power in these provinces. Even in the high-cost scenario, 36% of the energy demand from these nine coastal

provinces could be supplied by offshore wind. The economic benefits may be even more extensive in the future with a 200% energy surplus in the low-cost scenario, 116% with the higher cost option. Emphasizing the extent to which this is an untapped resource, offshore wind comprises currently only 1.6% of China's total wind power.

Trends in offshore wind

A number of studies have commented on the declining trend in China's onshore wind speeds (5–11). If slowing wind trends were to exist also for offshore, this could have a bearing on decisions as to whether conditions favorable for China at present could become unfavorable in the future, providing a possible negative incentive for future investments. Monthly CF trends are shown in Fig. 3 for the studied region and for mainland China over the 39-year period covered in this study. In contrast to the declining trend over much of the high-resource onshore wind area of mainland China indicated in the earlier studies, trends in offshore resources appear to have been more muted.

While there has been a slight decline in trends over much of the offshore region, environments further from the coast actually exhibit a slight positive bias. However, none of these trends for offshore wind power are statistically significant, except for the region off Fujian, a circumstance that may be due to the unique fact that the region is bordered to the east and west by land. Slowing wind speeds, therefore, are not considered of compelling concern for the future of China's offshore wind market.

Offshore wind variability and implications for grid flexibility

To illustrate the impact of integrating offshore wind power into local power systems, we summarize the temporal variations of power demand and wind power at an hourly and daily scale in Fig. 4 for Guangdong and Jiangsu provinces—the largest current offshore installations. The detailed variabilities of wind power at different time scales for all coastal provinces are summarized in fig. S2. Figure 4 (A and B) illustrates the daily variations of wind power and power demand throughout an entire year. Note that offshore wind power exhibits relatively minor seasonal variability, and the average CFs for offshore wind power in summer months are close to 30% in both Guangdong and Jiangsu provinces. In contrast, onshore wind power is highly seasonal in China, concentrated mainly in winter (21). The average CF for onshore wind

Table 1. Provincial physical offshore potential relative to demand. Mean potentials for offshore capacity and energy generation for different provinces over the studied period along with the demands for each province. The ratios of the corresponding quantities are also indicated. Provincial demand data were retrieved from NBS (32).

| Province	Offshore capacity (GW)	Offshore energy (TWh)	Peak demand (GW)	Energy demand (TWh)	Ratio offshore energy/demand
Fujian	308.8	1389.8	52.1	196.9	7.1
Guangdong	499.3	1584.4	104.6	561.0	2.8
Guangxi	111.7	310.3	41.2	136.0	2.3
Hainan	377.3	1227.0	7.5	28.7	43.8
Hebei	122.4	397.2	62.8	326.5	1.2
Jiangsu	462.7	1543.7	101.6	545.9	2.8
Liaoning	369.5	1336.6	62.8	203.7	6.6
Shandong	697.0	2334.8	109.4	539.1	4.3
Zhejiang	440.5	1725.6	83.3	387.3	4.5
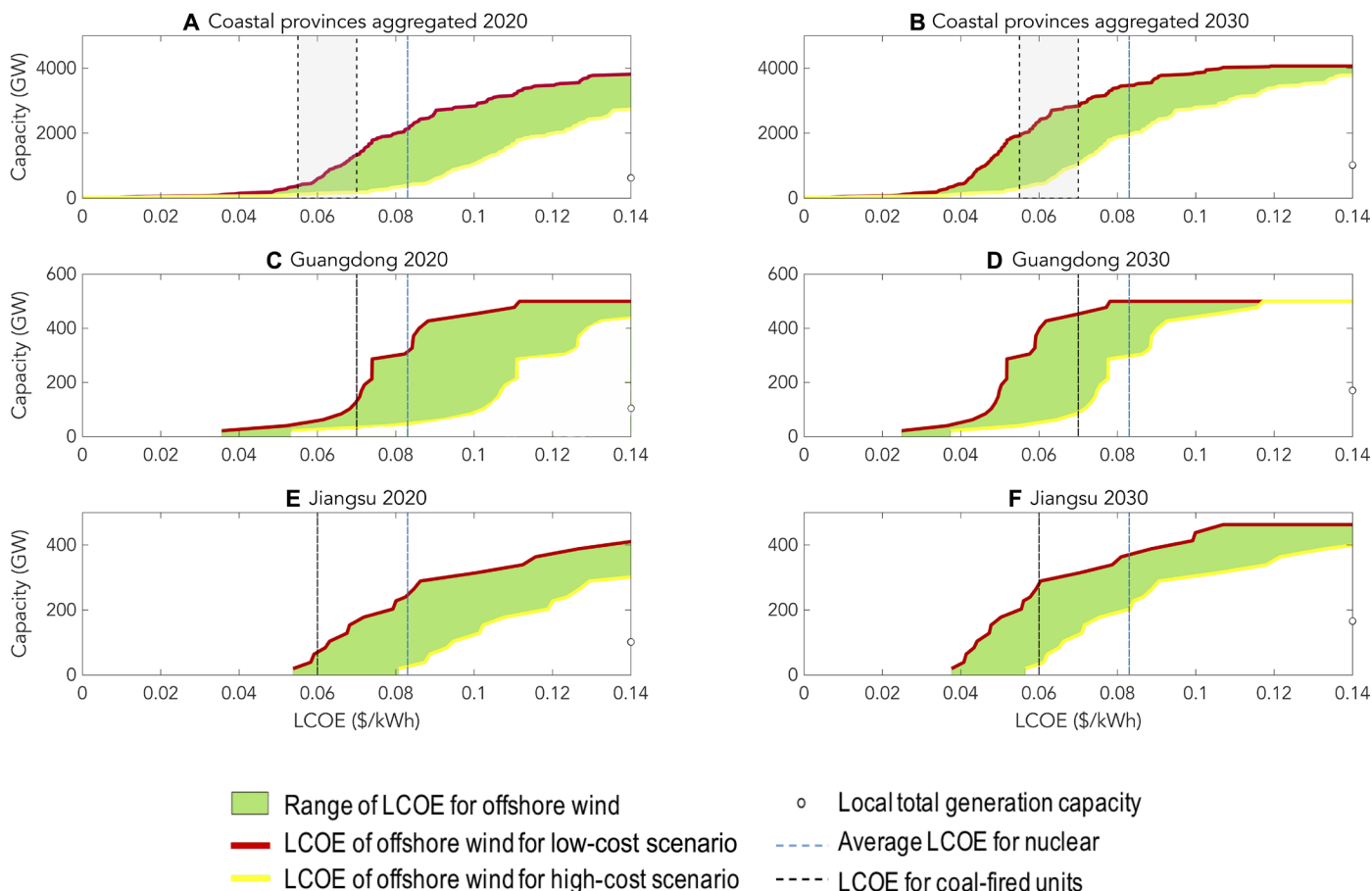
Fig. 2. Offshore wind supply curves. Estimated levelized costs for supply of power from offshore facilities for 2020 (**A**, **C**, and **E**) and 2030 (**B**, **D**, and **F**). The data cover an estimated low-cost (red line) and a potential higher-cost scenario (yellow line). The cost-competitive capacity is defined as the cumulative capacity that could be installed at an LCOE of less than $0.08 kWh^{-1}. For instance, Jiangsu could cost-competitively install roughly 30 GW of offshore wind with the high-cost scenario and roughly 200 GW in the low-cost scenario assuming costs that would apply currently in 2020.

power in the Beijing-Tianjin-Hebei area, for example, amounts to only 17% in summer.

The hourly variations of local power demand and offshore wind power are illustrated in Fig. 4 (C and D) for a typical week in Jiangsu and Guangdong provinces. Hourly variations of power demand for Guangdong are much greater than for Jiangsu. The fluctuations of offshore wind power for Guangdong are lower than the variations of power demand. The hour-to-hour ramping requirements in Guangdong and Jiangsu before and after integrating ~25% of offshore wind power are illustrated in Fig. 4 (E and F). The hourly rampings of power demand in Jiangsu lie mainly within the range of ±5 GW hour^{-1}; whereas the upward ramping for Guangdong peaks at 15 GW hour^{-1}, mainly during morning hours. After integrating ~25% of offshore wind power, the largest upward ramping for Jiangsu province exceeds 10 GW hour^{-1}; the upward ramping for Guangdong is affected to a lesser extent. Requirements for downward ramping will be increased substantially after integration of offshore wind power. The increase in ramping rates poses additional requirements for system flexibility.

Correlation coefficients between hourly variations of power demand and wind power were calculated on a daily basis throughout the year for all coastal provinces (with detailed provincial and seasonal statistics summarized in table S3). The seasonal and annual means of the daily correlation coefficients for Jiangsu and Guangdong are illus-

trated in Fig. 4 (G and H). The correlation coefficients for Jiangsu are positive for all seasons, with the highest values occurring in summer (0.18). The pattern indicates that offshore wind in Jiangsu tends to generate more power during peak hours. The correlation coefficients for Guangdong, in contrast, are highly seasonal: Offshore wind power is positively correlated with the daily variation of power demand in summer (0.19), transitioning to negative in winter (−0.11). We note that the hourly ramping and daily variations discussed above account only for the "within province" power demand. Possible power exports and interprovincial exchanges were not considered here explicitly. To optimally integrate a large contribution from offshore wind, it will be necessary to explore demand-side resources and storage technologies and to coordinate interprovincial transmission to provide needed system flexibility for coastal provinces over the long run.

DISCUSSION

The main purpose of this study was to evaluate China's potential for offshore wind. We used assimilated meteorological data from NASA's MERRA-2 to investigate offshore wind potential, temporal variability, trends, and cost estimates over the period 1980–2018.

The analysis reveals a number of key results, which could have important implications for China's future power system. First, China has

Table 2. Economic potential for provinces relative to demand. The mean economic potential for offshore energy generation (E in TWh) for different provinces over the studied period together with the ratio of economic energy generation to demand (R). The low- and high-cost scenarios are indicated for both present day and 2030. Note: *E* is the economic offshore energy generation for different provinces in TWh and *R* is the ratio of economic energy generation to provincial demand.

| Province	Economic 2020				Economic 2030			
	Low cost		High cost		Low cost		High cost	
	E	R	E	R	E	R	E	R
Fujian	853.0	4.2	344.7	1.7	1336.6	4.0	853	2.6
Guangdong	316.6	1.0	0.0	0.0	397.2	0.7	316.6	0.6
Guangxi	1139.5	2.1	99.8	0.2	1932.5	2.2	1054.2	1.2
Hainan	662.2	1.2	0.0	0.0	1119.7	1.3	576.1	0.6
Hebei	635.1	1.6	0.0	0.0	1231.6	2.0	533.9	0.8
Jiangsu	1341.1	6.8	388.9	2.0	1389.8	4.3	1341.1	4.2
Liaoning	902.9	1.6	147.9	0.3	1584.4	1.7	902.9	1.0
Shandong	164.7	1.2	106.4	0.8	310.2	1.4	164.5	0.7
Zhejiang	368.3	12.8	60.6	2.1	1059.4	22.7	284.4	6.1
Total	6383.4	2.0	1148.3	0.4	10,361.4	2.0	6026.7	1.2
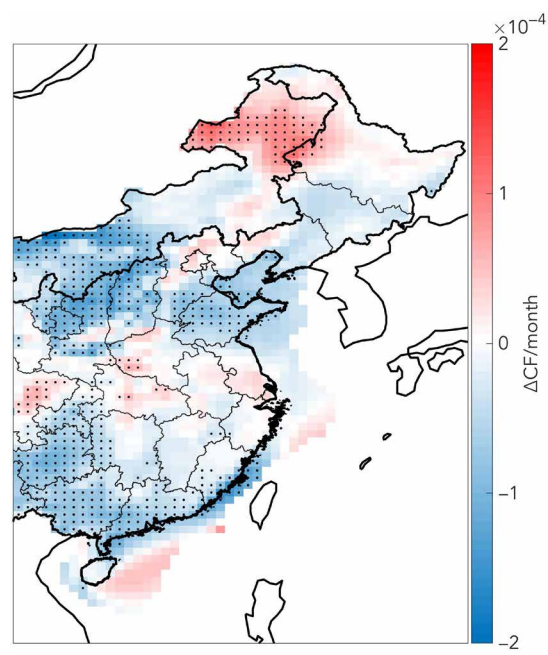
Fig. 3. Spatiotemporal trends in CF. Spatial distributions of CF trends (ΔCF/month) over the interval 1980–2018 for both onshore and offshore options. Trends that are significant at the 90th percentile are denoted with stippling.

important sources of offshore wind, with cumulative potentials for power production that greatly exceed the current demand for some of the most power-intensive provinces. Second, few significant declining trends in offshore wind were detected over the studied period using either MERRA-2 or ECMWF (European Centre for Medium-Range Weather Forecasts) assimilated meteorological data (see fig. S3). Considering the declining trends observed in both reanalysis and observational data for onshore winds, this result is encouraging and would appear to imply that China's offshore wind potential is unlikely to change

substantially under a warming climate. Third, China could currently harness offshore wind to supply as much as 36% of the total energy demand from the nine coastal provinces studied here at a cost-competitive price (LCOE ≤ $0.08 kWh^{-1}) even with the higher cost estimates assumed earlier. Fourth, integrating an important contribution of power from offshore sources poses little additional ramping requirements for Guangdong, although it could increase flexibility requirements for provinces such as Jiangsu. Efforts to improve power system flexibility should be addressed to accommodate contributions for offshore wind power in the future.

Despite these findings, there are a number of limitations that should be acknowledged. First, we used MERRA-2 assimilated meteorological data to investigate variations in China's offshore wind potential. While reanalysis products can reflect the general spatiotemporal variability, there may be issues of uncertainty for regions where data are sparse (*22*). Having said that, we found results that were consistent between MERRA-2 and ECMWF, which should mitigate any serious concerns associated with the use of MERRA-2 reanalysis data. Second, we noted a statistically significant declining trend for CFs off the coast of Fujian. Since this is a region with a large wind resource, it will be important for future studies to evaluate how Fujian's potential for offshore wind might be expected to change in the future under different climate scenarios. CMIP and large-ensemble models could be used to investigate this issue. Third, since the economics are becoming increasingly favorable for offshore wind power overall in China, it will be important to evaluate in detail how coastal power systems can accommodate variable power sources. Since the cost for storage systems is currently decreasing at a rapid rate, investment in storage facilities could provide additional opportunities that might help mitigate these variations. Demand response initiatives could also be effective. Further, the coastal provinces are increasingly interconnected. The national grid has invested in ultrahigh (1000 kV) voltage transmission lines, by which coastal provinces are tightly interconnected. Cities such as Shanghai could import offshore wind power through neighboring provinces, substituting in part for local fossil-fueled facilities. Variabilities in offshore wind power for different
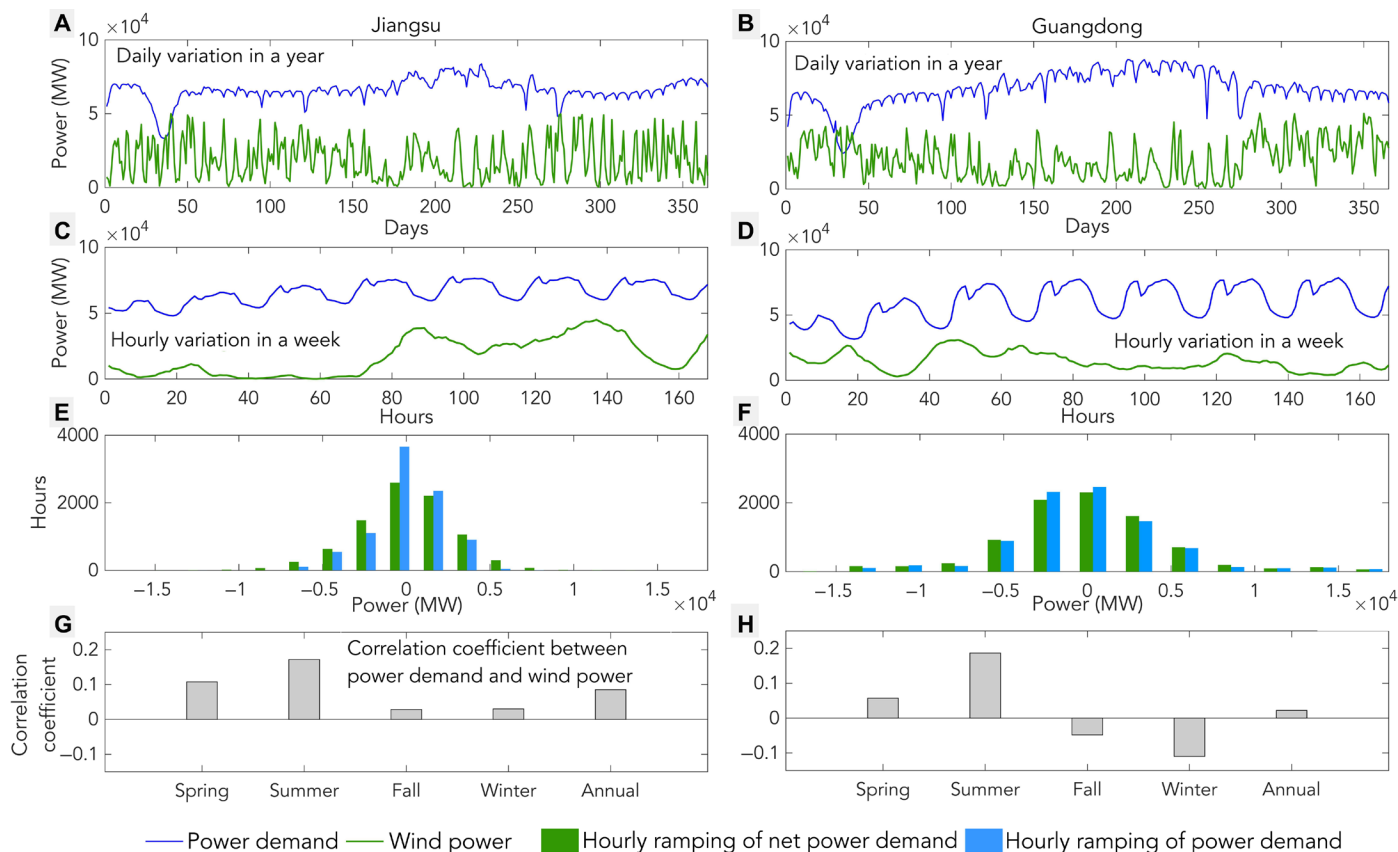
Fig. 4. Variation of wind power in the context of local power demand. (**A**) and (**B**) illustrate daily variation of power demand and wind power for Jiangsu and Guangdong provinces; (**C**) and (**D**) summarize hourly variations of power demand and wind power in a typical week for Guangdong and Jiangsu provinces; (**E**) and (**F**) indicate the frequency distribution of system ramping requirements with or without wind integration for Jiangsu and Guangdong, respectively. (**G**) and (**H**) indicate the seasonal and annual average correlation coefficients between daily variations of power demand and offshore wind generation for Jiangsu and Guangdong, respectively.

provinces can be mitigated further with better coordination of interprovincial transmission. The present analysis sheds some light on this. A follow-up analysis should explore the integration of future offshore wind into current power systems with detailed consideration of temporal variations in both supply and demand.

MATERIALS AND METHODS
Data overview
The wind data used in this study were taken from MERRA-2 (*23*), a NASA reanalysis product publicly available in NASA's Goddard Earth Sciences Data and Information Services Center. This database defines hourly wind speeds with a spatial resolution of 1/2° longitude by 2/3° latitude from 1980 to present. Hourly wind speeds at 100 m were extrapolated from 10 to 50 m using the vertical profile of the power law described by Archer and Jacobson (*24*). The friction coefficient in the analysis was evaluated using wind speeds represented at 10 and 50 m for each grid cell, as in Lu *et al.* (*25*). Wind power was computed on an hourly basis using the power curve for the MHI Vestas Offshore V164-8.0 MW wind turbine, a typical system used currently for offshore applications (specifications summarized in table S1). The ratio of hourly power output to the nameplate capacity of turbines was used to compute values of hourly CFs.

To determine locations suitable for offshore wind in China, we filtered data spatially based on a number of criteria. First, only loca-

tions within China's EEZ were considered. The EEZ is defined as the region under which a coastal state assumes jurisdiction over marine resources. The EEZ typically extends out to 200 nautical miles from shore, but differs when multiple countries lie within the 200–nautical mile range, for instance, North Korea and China in the Yellow Sea. China's boundaries for the EEZ were taken from Marine Regions, a database that aggregates information from a number of regional and national providers (*26*). Another filter that was adopted considered only offshore depths of less than or equal to 60 m. The offshore depth data used here were taken from the General Bathymetric Chart of the Oceans One Minute Grid, a global bathymetric grid providing data at a 1–arc min resolution (*27*). The MERRA-2 grid was rescaled to the high-resolution bathymetric data for appropriate integration of the two datasets. Note that we did not consider the potential for floating turbines, a relatively new innovation in the offshore wind industry that eliminates the 60-m depth limitation. This should not have a great bearing on our results, however, given that the waters in China's coastal environmental are shallow (<60 m) over much of the EEZ, and costs for installation of floating technology are currently elevated relative to those for fixed-bottom systems (*28*). Last, we removed areas from each grid point according to environments designated as either "Special Marine Reserves" (environmentally protected regions) or shipping routes. Areas for the Special Marine Reserves are defined in the National Marine Data and Information Service (*29*). SO_2 emissions from MERRA-2 were used as a surrogate for the identification

of shipping routes, and 20% of a cell's area was removed for locations defined as emitting SO_2 at a rate higher than 10^{-11} kg m^{-2} s^{-1}. This provides most likely an overestimate of the shipping impact; the spacing that we assumed to account for turbine-turbine interference was 1.1 km (as discussed below), and ships should be readily able to avoid obstructions imposed by this spacing. The area filtered according to these criteria is shown in fig. S4.

Provincial installed capacity, power generation, and LCOE estimates

Musial *et al.* (*30*) estimate that the spacing appropriate to minimize turbine-turbine interference for offshore wind is approximately 7 × 7 rotor diameters (1.04 km^2). The area for each latitude/longitude grid cell was divided by this value to compute the number of turbines that could fit maximally into a given cell. Note that this spacing does not account for the downstream wake effect, which is too small scale of a phenomenon to be modeled accurately using the MERRA-2 data. Given that the average downstream power loss is on the order of 5% (*31*), the wake effect should not have a significant bearing on the present results. The potential installed capacity (in gigawatts) is computed by multiplying the number of turbines in a cell by the turbine power (8 MW in this case).

The next step is to quantify the offshore power that could be supplied to individual provinces. To do this, we assumed that the offshore wind resource available over a given location in China's EEZ was under the jurisdiction of the country's nearest province. These provincial divisions, along with the mean and SD of the CF over the period 1980–2018, are indicated in Fig. 1. From the installed capacity and CF data, estimates of available energy *E(lat,lon,t)* (in kilowatt-hours) were computed using the equation

$$E(lat, lon, t) = CF(lat, lon, t) \times C(lat, lon) \times 8760 \quad (1)$$

where *C(lat,lon)* represents the installed capacity at a given location, *CF(lat,lon,t)* is the CF at the location, and 8760 defines the number of hours in a year. The potential capacities and power yields are compared on a provincial basis with capacity and energy demands using data from the National Bureau of Statistics (NBS) (*32*). The demand data were projected to the year 2030, assuming a 5% annual growth.

The LCOE is a measure of the per-unit cost, expressed typically in U.S. cents kWh^{-1}. Mathematically, LCOE is defined as the ratio of the cumulative costs over time to the cumulative energy generated over this period. Here, we compute the offshore LCOE in 2020 for each location under two current capital cost scenarios: (i) high cost ($3500 kW^{-1}) and (ii) low cost ($2000 kW^{-1}). Costs for each scenario were obtained by taking the range of installed costs for offshore wind farms in 2018 as indicated in IRENA (*2*). These baseline costs were adjusted spatially according to depth and distance to shore. Using results from Maness *et al.* (*33*), we developed a linear regression model to derive relationships between the various parameters (depth and distance to shore) and baseline costs. The baseline costs C_0 ($ kW^{-1}) were adjusted on the basis of depth *d* (m) and distance from shore *S* (m) according to the equation

$$C(d, S) = C_o \times (0.0084d + 0.8368) \times (0.0057S + 0.7714) \quad (2)$$

This equation represents a simplified version of the results from Maness *et al.* (*33*), which include a robust analysis accounting for how depth and distance from shore influenced costs associated with substructure, foundation, infrastructure, engineering, and installation. The amortized cost, *I(lat,lon)*, is computed then using the equation

$$I(lat, lon) = AC(lat, lon) \times r \times \frac{(1 + r)^y}{(1 + r)^y - 1} \quad (3)$$

where *AC(lat,lon)* is the cost adjusted for depth and distance to shore, *r* is the interest rate (8%), and *y* is the assumed payback period (20 years). The LCOE at a given location is calculated according to

$$LCOE(lat, lon) = \frac{I(lat, lon)}{CF_{MEAN}(lat, lon) \times 8760} \quad (4)$$

where $CF_{MEAN}(lat, lon)$ is the mean CF and 8760 is the number of hours in a year. These costs were projected to 2030, using the 30% LCOE median decrease based on the recommendations from Wiser *et al.* (*20*).

We arranged spatial LCOE values from smallest to largest, integrating on a province-by-province basis to obtain estimates of relevant cost curves. These curves were compared (Fig. 4) with provincial costs for current power generation technologies (nuclear and coal-fired power plants). The nuclear LCOE estimates are taken from Xu *et al.* (*34*), and coal-fired power plant estimates are from Shu-Chuan (*35*). We identified the LCOE for cost-competitive offshore wind as $0.08 kWh^{-1}.

SUPPLEMENTARY MATERIALS

Supplementary material for this article is available at http://advances.sciencemag.org/cgi/content/full/6/8/eaax9571/DC1

Fig. S1. Spatial distribution of the CF standard deviation over 1980–2018 within China's EEZ.
Fig. S2. Fourier decomposition of offshore wind variability in different provinces.
Fig. S3. Spatial distributions of CF trends [CF month −1] over 1979–2018 for the filtered region and onshore for ECMWF.
Fig. S4. Spatial distributions of the offshore wind constraints used in the filtering process.
Table S1. Maximum and minimum monthly energy potential (TWh) for each coastal province studied here.
Table S2. Specifications for the MHI Vestas Offshore V164-8.0 MW turbines.
Table S3. Averaged daily correlation coefficients between hourly power demand and wind generation for different provinces and seasons.

REFERENCES AND NOTES

1. X. Chen, J. Lv, M. B. McElroy, X. Han, C. P. Nielsen, J. Wen, Power system capacity expansion under higher penetration of renewables considering flexibility constraints and low carbon policies. *IEEE Trans. Power Syst.* **33**, 6240–6253 (2018).
2. International Renewable Energy Agency (IRENA) 2018, Renewable Power Generation Costs in 2017; www.irena.org/publications/2018/Jan/Renewable-power-generation-costs-in-2017 [accessed 21 March 2019].
3. Y. Qi, J. Lu, M. Zhu, Wind curtailment in China and lessons from the United States. Brookings Institution 2018; www.brookings.edu/research/wind-curtailment-in-china-and-lessons-from-the-united-states/ [accessed 20 March 2019].
4. N. Zhang, X. Lu, M. B. McElroy, C. P. Nielsen, X. Chen, Y. Deng, C. Kang, Reducing curtailment of wind electricity in China by employing electric boilers for heat and pumped hydro for energy storage. *Appl. Energy* **184**, 987–994 (2016).
5. P. Sherman, X. Chen, M. B. McElroy, Wind-generated electricity in China: Decreasing potential, inter-annual variability and association with changing climate. *Sci. Rep.* **7**, 16294 (2017).
6. Z.-Z. Hu, L. Bengtsson, K. Arpe, Impact of global warming on the Asian winter monsoon in a coupled GCM. *J. Geophys. Res. Atmos.* **105**, 4607–4624 (2000).
7. M. E. Hori, H. Ueda, Impact of global warming on the East Asian winter monsoon as revealed by nine coupled atmosphere-ocean GCMs. *Geophys. Res. Lett.* **33**, L03713 (2006).
8. M. Kimoto, Simulated change of the East Asian circulation under global warming scenario. *Geophys. Res. Lett.* **32**, L16701 (2005).
9. Z.-Z. Hu, S. Yang, R. Wu, Long-term climate variations in China and global warming signals. *J. Geophys. Res. Atmos.* **108**, 4614 (2003).
10. F. Panagiotopoulos, M. Shahgedanova, A. Hannachi, D. B. Stephenson, Observed trends and teleconnections of the siberian high: A recently declining center of action. *J. Clim.* **18**, 1411–1422 (2005).

11. R. D'Arrigo, G. Jacoby, R. Wilson, F. Panagiotopoulos, A reconstructed Siberian High index since A.D. 1599 from Eurasian and North American tree rings. *Geophys. Res. Lett.* **32**, L05705 (2005).

12. Y. Jiang, Y. Luo, Z. Zhao, S. Tao, Changes in wind speed over China during 1956–2004. *Theor. Appl. Climatol.* **99**, 421–430 (2009).

13. K. B. Karnauskas, J. K. Lundquist, L. Zhang, Southward shift of the global wind energy resource under high carbon dioxide emissions. *Nat. Geosci.* **11**, 38–43 (2017).

14. IRENA, REthinking Energy: Towards a new power system. International Renewable Energy Agency 2014; www.irena.org/publications/2014/Sep/REthinking-Energy-Towards-a-new-power-system [accessed 21 March 2019].

15. International Renewable Energy Agency (IRENA) 2018, Renewable Energy Statistics 2018; www.irena.org/publications/2018/Jul/Renewable-Energy-Statistics-2018 [accessed 21 March 2019].

16. J. Kumagai, With vineyard wind, the U.S. finally goes big on offshore wind power. IEEE spectrum: Technology, engineering, and science news 2019; https://spectrum.ieee.org/energy/renewables/with-vineyard-wind-the-us-finally-goes-big-on-offshore-wind-power [accessed 22 March 2019].

17. M. R. Davidson, D. Zhang, W. Xiong, X. Zhang, V. J. Karplus, Modelling the potential for wind energy integration on China's coal-heavy electricity grid. *Nat. Energy* **1**, 16086 (2016).

18. X. Lu, M. B. McElroy, X. Chen, C. Kang, Opportunity for offshore wind to reduce future demand for coal-fired power plants in china with consequent savings in emissions of CO_2. *Environ. Sci. Technol.* **48**, 14764–14771 (2014).

19. L. Hong, B. Möller, Offshore wind energy potential in China: Under technical, spatial and economic constraints. *Energy* **36**, 4482–4491 (2011).

20. R. Wiser, K. Jenni, J. Seel, E. Baker, M. Hand, E. Lantz, A. Smith, Expert elicitation survey on future wind energy costs. *Nat. Energy* **1**, 16135 (2016).

21. X. Chen, M. B. McElroy, C. Kang, Integrated energy systems for higher wind penetration in China: Formulation implementation and impacts. *IEEE Trans. Power Syst.* **33**, 1309–1319 (2018).

22. M. Schwartz, R. George, D. Elliott, *The Use of Reanalysis Data for Wind Resource Assessment at the National Renewable Energy Laboratory* (European Wind Energy Conference, 1999).

23. R. Gelaroa, W. McCarty, M. J. Suárez, R. Todling, A. Molod, L. Takacs, C. A. Randles, A. Darmenov, M. G. Bosilovich, R. Reichle, K. Wargan, L. Coy, R. Cullather, C. Draper, S. Akella, V. Buchard, A. Conaty, A. M. da Silva, W. Gu, G. K. Kim, R. Koster, R. Lucchesi, D. Merkova, J. E. Nielsen, G. Partyka, S. Pawson, W. Putman, M. Rienecker, S. D. Schubert, M. Sienkiewicz, B. Zhao, The modern-era retrospective analysis for research and applications, version 2 (MERRA-2). *J. Clim.* **30**, 5419–5454 (2017).

24. C. L. Archer, M. Z. Jacobson, Evaluation of global wind power. *J. Geophys. Res. Atmos.* **200**, D12110 (2005).

25. X. Lu, M. B. McElroy, C. P. Nielsen, X. Chen, J. Huang, Optimal integration of offshore wind power for a steadier, environmentally friendlier, supply of electricity in China. *Energy Policy* **62**, 131–138 (2013).

26. Flanders Marine Institute. Maritime Boundaries Geodatabase: Maritime Boundaries and Exclusive Economic Zones (200NM), version 10. 2018. doi:10.14284/312.

27. J. J. Becker, D. T. Sandwell, W. H. F. Smith, J. Braud, B. Binder, J. Depner, D. Fabre, J. Factor, S. Ingalls, S.-H. Kim, R. Ladner, K. Marks, S. Nelson, A. Pharaoh, R. Trimmer, J. Von Rosenberg, G. Wallace, P. Weatherall, Global bathymetry and elevation data at 30 arc seconds resolution: SRTM30_PLUS. *Mar. Geod.* **32**, 355–371 (2009).

28. P. Beiter, W. Musial, L. Kilcher, M. Maness, A. Smith, An Assessment of the Economic Potential of Offshore Wind in the United States from 2015 to 2030. Tech. Rep. (NREL/TP-6A20-67675, 2017).

29. National Marine Data and Information Service, Environmental Protection Areas. National Marine Science Data Sharing Service Platform 2018; http://www.nmdis.org.cn/english/nmdiss-mission/ [accessed 1 May 2019].

30. W. Musial, D. Heimiller, P. Beiter, G. Scott, C. Draxl, 2016 Offshore Wind Energy Resource Assessment for the United States. Tech. Rep. (NREL/TP-5000-66599, 2016).

31. Q. Wang, K. Luo, R. Yuan, S. Zhang, J. Fan, Wake and performance interference between adjacent wind farms: Case study of Xinjiang in China by means of mesoscale simulations. *Energy* **166**, 1168–1180 (2019).

32. National Bureau of Statistics (NBS) 2002–2018, *China Energy Statistical Yearbook 2001–2018* (China Statistical Press, 2018).

33. M. Maness, B. Maples, A. Smith, NREL Offshore Balance-of-System Model. Tech. Rep. (NREL/TP-6A20-66874, 2017).

34. Y. Xu, J. Kang, J. Yuan, The prospective of nuclear power in China. *Sustainability* **10**, 2086 (2018).

35. W. Shu-Chuan, The latest electricity prices, resources and power generation data of the provinces, and the materials used for the parity online projects are all available, Sgcio.com 2018; www.sgcio.com/news/haiwaidianli/2018/1026/100550.html [accessed 21 March 2019].